Short Article

Molecular Cell

Mre11-Sae2 and RPA Collaborate to Prevent Palindromic Gene Amplification

Graphical Abstract

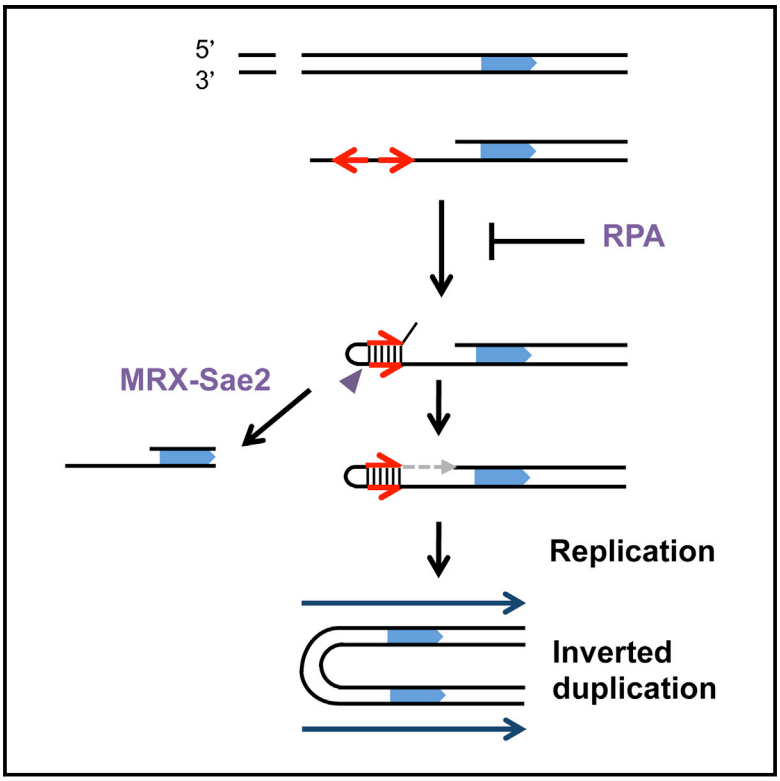

Authors

Sarah K. Deng, Yi Yin, Thomas D. Petes, Lorraine S. Symington

Correspondence

lss5@cumc.columbia.edu

In Brief

In this study, Deng et al. present evidence in support of a foldback priming mechanism to generate palindromic duplications in yeast. This class of chromosome rearrangements is normally prevented by RPA, which inhibits intra-strand annealing between short repeats, and by the hairpin-cleaving activity of the Mre11 nuclease and Sae2.

Highlights

- Short inverted repeats drive formation of large palindromic duplications
- RPA inhibits annealing of inverted repeats to restrict hairpin formation
- Mre11-Sae2 opens hairpins to prevent formation of palindromic duplications
- The hairpin-capped chromosome is replicated to form an unstable dicentric chromosome

Deng et al., 2015, Molecular Cell *60*, 500–508
November 5, 2015 ©2015 Elsevier Inc.
http://dx.doi.org/10.1016/j.molcel.2015.09.027

CellPress

Molecular Cell
Short Article

Mre11-Sae2 and RPA Collaborate to Prevent Palindromic Gene Amplification

Sarah K. Deng,[1] Yi Yin,[2] Thomas D. Petes,[2] and Lorraine S. Symington[1,*]
[1]Department of Microbiology & Immunology, Columbia University Medical Center, New York, NY 10032, USA
[2]Department of Molecular Genetics and Microbiology, Duke University Medical Center, Durham, NC 27710, USA
*Correspondence: lss5@cumc.columbia.edu
http://dx.doi.org/10.1016/j.molcel.2015.09.027

SUMMARY

Foldback priming at DNA double-stranded breaks is one mechanism proposed to initiate palindromic gene amplification, a common feature of cancer cells. Here, we show that small (5–9 bp) inverted repeats drive the formation of large palindromic duplications, the major class of chromosomal rearrangements recovered from yeast cells lacking Sae2 or the Mre11 nuclease. RPA dysfunction increased the frequency of palindromic duplications in Sae2 or Mre11 nuclease-deficient cells by ~1,000-fold, consistent with intra-strand annealing to create a hairpin-capped chromosome that is subsequently replicated to form a dicentric isochromosome. The palindromic duplications were frequently associated with duplication of a second chromosome region bounded by a repeated sequence and a telomere, suggesting the dicentric chromosome breaks and repairs by recombination between dispersed repeats to acquire a telomere. We propose secondary structures within single-stranded DNA are potent instigators of genome instability, and RPA and Mre11-Sae2 play important roles in preventing their formation and propagation, respectively.

INTRODUCTION

Diverse and complex chromosome rearrangements, including inter-chromosomal translocations, deletions, and gene amplifications, are often found in the genomes of cancer cells (Stephens et al., 2011). Intra-chromosomal gene amplifications are organized as direct or inverted (palindromic) duplications and can confer a growth advantage to promote tumor initiation, metastatic dissemination or drug resistance resulting in treatment failure (Kitada and Yamasaki, 2007, 2008; Marotta et al., 2012; Slamon et al., 1987; Tanaka and Yao, 2009). Palindromic duplications have been identified in metastatic pancreatic cancer and ErbB-2 (HER2) positive breast cancers (Campbell et al., 2010; Marotta et al., 2012; Slamon et al., 1987; Waddell et al., 2015).

Mechanisms used to explain palindromic amplification commonly invoke a dicentric isochromosome that undergoes breakage-fusion-bridge (BFB) cycles (Marotta et al., 2013; Narayanan et al., 2006; Tanaka and Yao, 2009). A dicentric isochromosome can be formed by fusion of the sister chromatids produced by replication of a chromosome broken in the G1 phase of the cell cycle, or with dysfunctional telomeres (Figure S1). Asymmetric breakage of the dicentric chromosome during mitosis results in inverted duplication close to the breakpoint, further BFB cycles can result in extensive gene amplification. A role for inverted repeats was first proposed to explain the formation of short, linear palindromic chromosomes during nuclear differentiation of Tetrahymena (Yasuda and Yao, 1991). A 42-bp inverted repeat was shown to be essential for palindrome formation, and a subsequent study supported a model whereby annealing of the repeats after end resection from a double-strand break (DSB) creates a hairpin-capped molecule that is replicated to generate the palindromic duplication (Figure S1) (Butler et al., 1996). Short inverted repeats have also been shown to mediate palindromic gene amplification in yeast and mammalian cells (Butler et al., 1996; Maringele and Lydall, 2004; Marotta et al., 2013; Putnam et al., 2014; Rattray et al., 2005; Tanaka et al., 2002). In yeast, the recovery of palindromic duplications is markedly increased in cells lacking Sae2 or expressing a nuclease-defective mutant form of Mre11 (Rattray et al., 2001, 2005). Sae2 activates the Mre11-Rad50-Xrs2 (MRX) complex to cleave the 5′ strand internal to the DSB end to initiate 5′-3′ DNA end resection and promotes opening of hairpin-capped DNA ends (Cannavo and Cejka, 2014; Lengsfeld et al., 2007; Lobachev et al., 2002).

Long inverted repeats (>300 bp) function as fragile sites in yeast and stimulate gross chromosome rearrangements (GCRs), including dicentric/acentric chromosome formation, non-reciprocal translocation, and gene amplification (Lemoine et al., 2005; Lobachev et al., 2002; Mizuno et al., 2009; Narayanan et al., 2006; Paek et al., 2009). Inverted repeats are thought to extrude to form a cruciform or hairpin structure that is cleaved at the base to create DSBs terminated by covalently closed hairpins; alternatively, intramolecular annealing of inverted repeats exposed by end resection of a DSB could create a hairpin-capped end (Darmon et al., 2010). Failure to resolve the hairpin-capped ends by MRX and Sae2 (or SbcCD in *Escherichia coli*) leads to the formation of acentric and dicentric palindromic molecules that can undergo further rearrangement (Darmon et al., 2010; Eykelenboom et al., 2008; Lobachev et al., 2002; Narayanan et al., 2006). Recombination-dependent replication fork restart within inverted repeats at a stalled replication fork can also result in dicentric/acentric palindromic chromosome rearrangements (Mizuno et al., 2009).

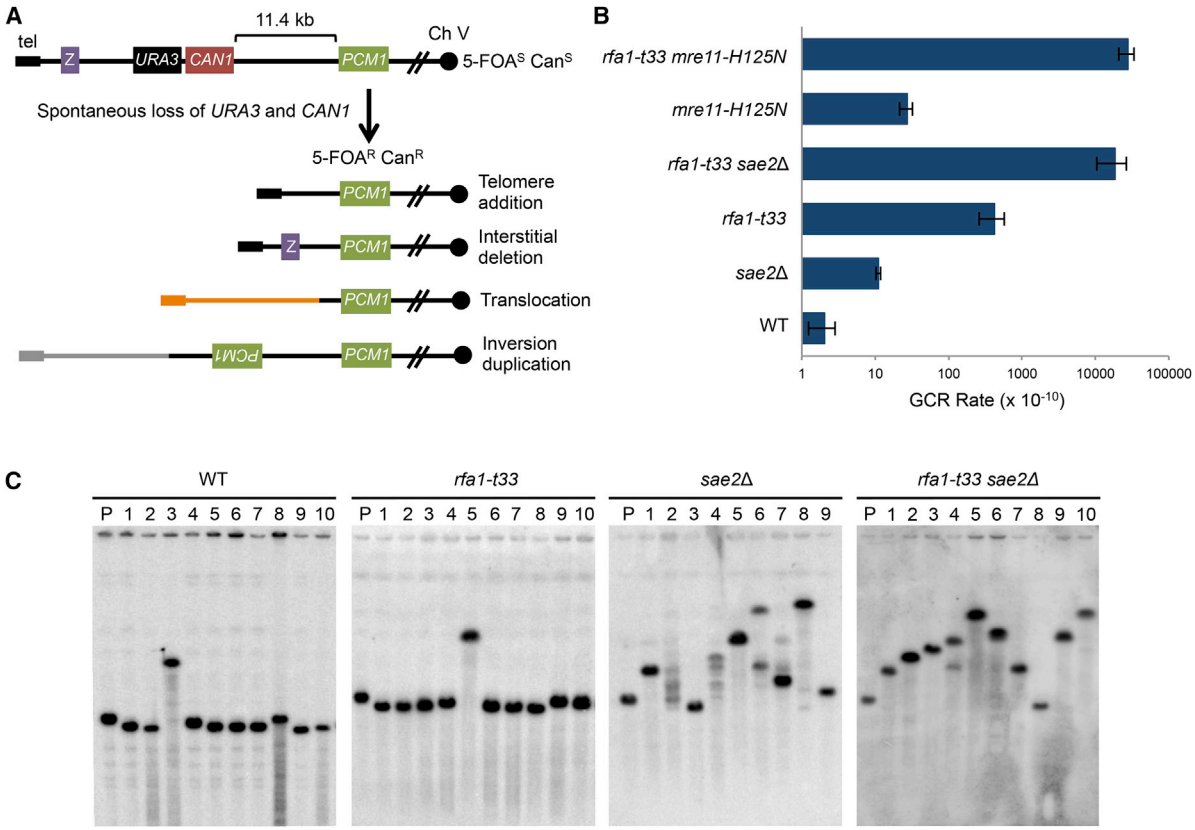

Figure 1. Increased GCR Rate and an Altered Spectrum of Events in *sae2*Δ Derivatives

(A) Schematic of the GCR assay and rearrangements. Z indicates a distal Ch V gene that would be retained after interstitial deletion, and the solid circles denote the centromere. Orange and gray lines indicate translocated sequences.

(B) GCR rates for the indicated genotypes. WT, wild-type. The rates shown are the average of three independent trials for WT, *sae2*Δ, *mre11-H125N*, *rfa1-t33 mre11-H125N*, and five and seven independent trials for *rfa1-t33* and *rfa1-t33 sae2*Δ, respectively. Error bars, SD.

(C) PFGE of WT, *rfa1-t33*, *sae2*Δ, and *rfa1-t33 sae2*Δ GCR clones. The first lane of each blot (P) shows the parental un-rearranged Ch V.

See also Figures S1 and S2.

Conditions that favor annealing between short homologies are expected to increase foldback priming resulting in palindromic duplications. Replication protein A (RPA), the main eukaryotic single-stranded DNA (ssDNA) binding protein, removes secondary structure from ssDNA and prevents annealing between short oligonucleotides in vitro (Gibb et al., 2012; Sugiyama et al., 1998). Depletion of Rfa1 (*RFA1*/*RPA1* encodes the largest subunit of the heterotrimeric RPA complex) from yeast cells results in the formation of foldback structures by annealing between short inverted repeats within the ssDNA formed by end resection at DSBs (Chen et al., 2013). Furthermore, expression of hypomorphic alleles of *RFA1*, which encode proteins with reduced DNA binding activity, greatly increases the frequency of microhomology-mediated end joining (MMEJ), suggesting that RPA binding to ssDNA prevents annealing between short homologies that can result in genome destabilization (Deng et al., 2014).

Because depletion of RPA from cells results in foldback structures at DSBs, we were interested in whether *rfa1* hypomorphic mutants would exhibit an increased frequency of palindromic duplication. We found that naturally occurring short inverted repeats (5–9 bp) stimulate formation of large (51–83 kb) palindromic duplications, which are the main class of GCRs recovered from *sae2*Δ and *mre11-H125N* mutants. Although palindromic duplications were not found among the GCRs from the *rfa1-t33* mutant, the frequency of these events was increased ~1,000-fold in the *rfa1-t33 sae2*Δ and *rfa1-t33 mre11-H125N* double mutants relative to the *sae2*Δ and *mre11-H125N* mutants. We also recovered rearrangements from the *rfa1-t33 sae2*Δ mutant that had a more than 2-fold amplification, similar to amplifications observed in tumor cells.

RESULTS

rfa1-t33 and *sae2*Δ Synergistically Increase the GCR Rate

To examine genomic instability caused by *rfa1-t33* and *sae2*Δ mutations, we used a well-characterized assay that measures the accumulation of spontaneous GCRs on the left arm of chromosome V (Ch V) by simultaneous loss of the *URA3* and *CAN1* genes (Figure 1A) (Chen and Kolodner, 1999). This assay detects a broad spectrum of GCR events with the frequency indicative of general genome stability and distinct repair products recovered

Table 1. Spectrum of GCR Events

Relevant Genotype	Can^R 5-FOA^R Mutation Rate[a]	Isolates Analyzed	Telomere Addition	Deletion/ Translocation	Ch V Left Arm Duplication (class I, class II)
WT	2.04 [±0.72] × 10^{-10} (1.0)	12[b]	9	1	1 (1, 0)
*sae2*Δ	1.11 [±0.08] × 10^{-9} (5.4)	9	1	1	7 (4, 3)
mre11-H125N	2.70 [±0.46] × 10^{-9} (13.2)	10	2	0	8 (6, 2)
rfa1-t33	4.20 [±1.80] × 10^{-8} (205)	14	7	7	0 (0, 0)
*rfa1-t33 sae2*Δ	1.86 [±1.10] × 10^{-6} (9,079)	10	1	0	9 (9, 0)
rfa1-t33 mre11-H125N	2.75 [±0.57] × 10^{-6} (13,436)	10	3	0	7 (3, 4)

Class I, Duplication on Ch V and second homology dependent invasion; class II, duplication on Ch V only.
See also Figure S3.
[a]Rate of accumulating Can^R 5-FOA^R progeny. Numbers in brackets indicate SD. The number in parenthesis is the fold increase relative to WT.
[b]One WT GCR clone contained a point mutation in the *CAN1* gene and no discernable mutation at *URA3*. This clone was able to grow on 5-FOA-containing and SC-URA media.

being reflective of the inherent nature of the genotype (Putnam et al., 2005). The *rfa1-t33* mutant was chosen for this study because the RPA^{t33} mutant protein is partially defective for removal of secondary structure from ssDNA in vitro (Deng et al., 2014). The *rfa1-t33* mutant showed a 205-fold increased rate of GCR accumulation compared to WT, consistent with a previous study (Figure 1B; Table 1) (Chen and Kolodner, 1999). Although loss of Sae2 resulted in only a 5-fold increase in the GCR rate, a synergistic increase was observed in the *rfa1-t33 sae2*Δ double mutant (1.86 × 10^{-6}, 9,000-fold elevation).

The large increase in the frequency of GCRs in the *rfa1-t33* mutant could be due to more initiating lesions, defective homologous recombination (HR), or an altered mode of repair. We found the GCR rate of the HR-defective *rad51*Δ mutant was increased by only 4-fold relative to WT, and while the *sae2*Δ mutation did synergize with *rad51*Δ, the rate of GCRs was ~100-fold lower than the *rfa1-t33 sae2*Δ double mutant (Figure S2A). An increased number of spontaneous lesions would be expected to increase the rate of deletions between direct repeats. We found a small but significant increase in the rate of deletions in the *rfa1-t33* mutant ($p = 0.05$), consistent with more initiating lesions, while the rate of spontaneous Rad51-dependent gene conversion was comparable to WT cells (Figure S2B). Thus, the increased GCR rate of the *rfa1-t33* mutant is not a consequence of impaired HR and is likely due to aberrant repair of replication-associated DNA breaks.

GCRs Recovered from *sae2*Δ Derivatives Have an Expanded Chromosome V

To determine the spectrum of GCRs, we first examined Ch V by pulsed-field gel electrophoresis (PFGE) and Southern blot hybridization using a *PCM1* probe, an essential gene on Ch V. We found that the majority of rearrangements in WT and the *rfa1-t33* mutant resulted in a Ch V species with a faster mobility than the parental Ch V (Figure 1C). In contrast, the majority of *sae2*Δ and *rfa1-t33 sae2*Δ GCR clones exhibited an expanded Ch V as evidenced by the slower mobility by PFGE (Figure 1C). Some *sae2*Δ GCR isolates displayed a smear of Ch V products indicating either a mixed population of repaired products or an unstable Ch V.

To better understand the types of GCRs in the *rfa1-t33* and *sae2*Δ derivatives, we utilized a previously described method to identify the location of the breakpoint by overlap PCR using Ch V primers and then attempted to sequence across the junction using an arbitrary PCR strategy (Figure S3) (Schmidt et al., 2006). We characterized 12 GCR isolates from WT cells and found that repair occurred primarily by telomere addition (Table 1). We were unable to identify the breakpoint junction by PCR of the GCR clone with an expanded Ch V; this event was further characterized by array comparative genome hybridization (aCGH, see below). Of 14 GCR clones analyzed from the *rfa1-t33* mutant, we found that seven were due to telomere addition, two events were due to translocations, and five events were interstitial deletions mediated by microhomologies (Table 1). Telomere addition and interstitial deletion are consistent with a shorter Ch V species by PFGE, while the translocation events exhibited an expanded Ch V. The spectra of GCR events found for WT and the *rfa1-t33* mutant are consistent with a previous study (Chen and Kolodner, 1999).

Rearrangements in *sae2*Δ Mutants Result from Inverted Duplication of Ch V

Of the nine GCR clones analyzed from the *sae2*Δ mutant, one resulted from telomere addition and another was due to a translocation mediated by microhomologies. For the remaining seven events, we identified the breakpoints but could not amplify the rearrangement junctions by PCR. Similarly, one of ten GCR clones from the *rfa1-t33 sae2*Δ mutant was due to telomere addition, and we failed to amplify junctions from the other nine clones. Since previous studies had shown recovery of palindromic duplications from *sae2*Δ mutants (Putnam et al., 2014; Rattray et al., 2001, 2005), it seemed likely that the failure to amplify junctions from the majority of *sae2*Δ and *rfa1-t33 sae2*Δ GCR clones was due to the presence of inverted duplications, which are difficult to amplify as a result of snapback structures formed during PCR.

Two strategies were used to determine the structure of the rearrangements. First, we physically mapped the region around the breakpoint of several GCR clones by restriction digestion of genomic DNA and hybridization with appropriate probes (Figure 2A). The distance between each restriction endonuclease

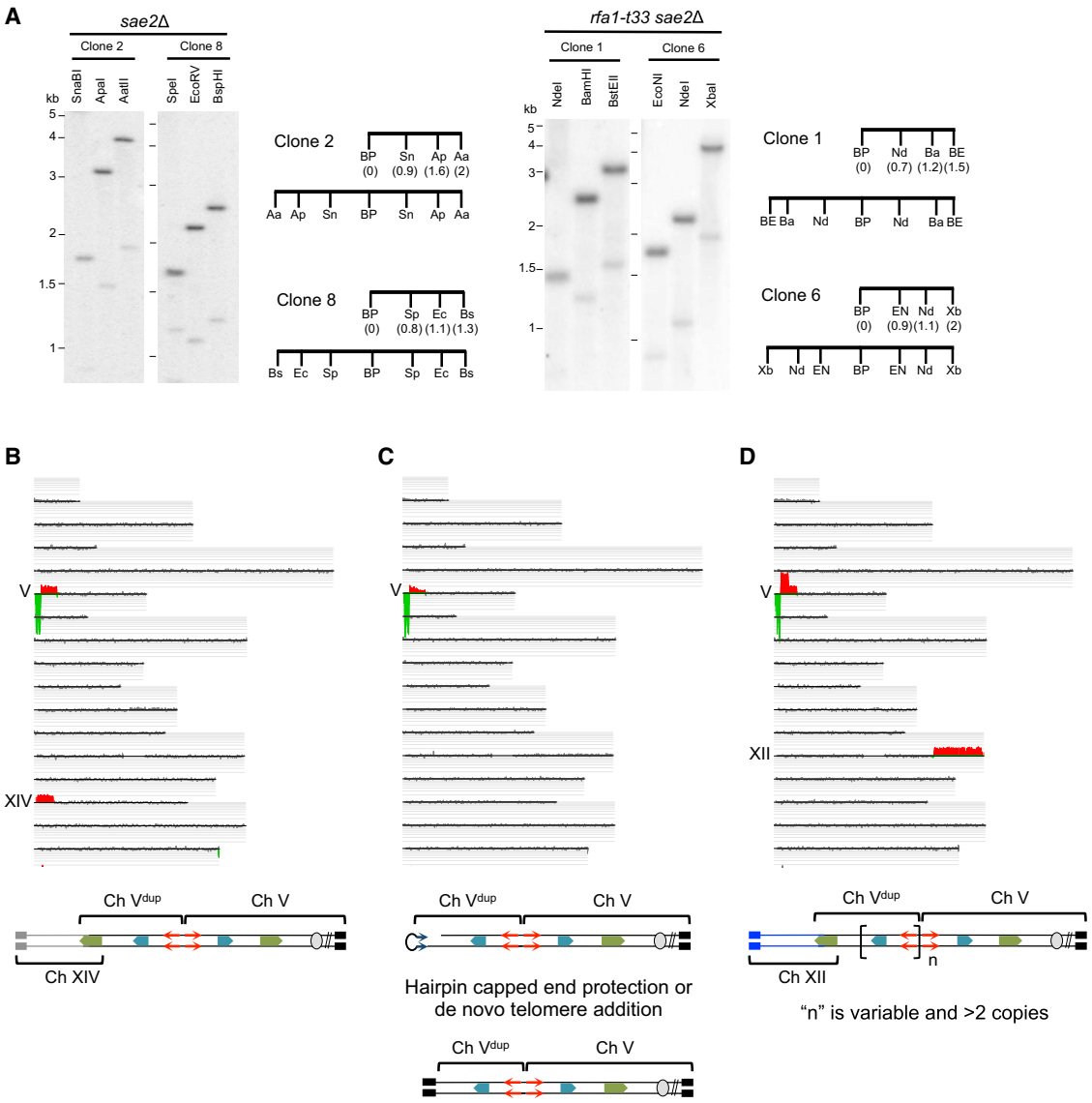

Figure 2. Inversion Duplications Are Recovered from *sae2*Δ Derivatives after Chromosomal Rearrangement

(A) Physical analysis of the breakpoint region surrounding the DSB. Schematic shows location of the breakpoint (BP) and restriction enzyme recognition sites adjacent to the BP. For each pair of lines, the top line shows the sites for the control strain, and the bottom line shows the sites in the strain with the chromosome rearrangement. Abbreviations for restriction enzymes are as follows: SnaBI (Sn) ApaI (Ap), AatII (Aa), SpeI (Sp), EcoRV (Ec), BspHI (Bs), NdeI (Nd), BamHI (Ba), BstEII (BE), EcoNI (EN), XbaI (Xb).

(B–D) aCGH analysis of GCR clones. Schematics to show the rearranged ChV derived from the aCGH data are shown below the plots. Solid green indicates a Ty-related or tRNA element. Blue represents gene X within the duplicated region.

(B) Representative aCGH from a *sae2*Δ GCR clone indicating deletion of the terminal fragment of Ch V, duplication adjacent to the breakpoint on Ch V and an additional duplication to create non-reciprocal translocation. Each horizontal line represents each yeast chromosome (I–XVI), and the roman numerals to the left indicate the chromosomes with alterations. Green below the line, sequence loss; red above the line, sequence gain.

(C) Representative aCGH from a *sae2*Δ GCR clone showing duplication adjacent to the break on Ch V only.

(D) Representative aCGH from a *rfa1-t33 sae2*Δ GCR clone with a higher-order amplification adjacent to the breakpoint.

See also Figure S3.

site chosen and the breakpoint is defined as distance “X”, and we reasoned that if a palindromic duplication had occurred we would recover DNA fragments of size 2X because the restriction site would be duplicated on the other side the breakpoint. We used several restriction endonucleases that were predicted to cleave at varying distances from the breakpoint, and all showed a fragment of twice the expected size, consistent with a palindromic duplication. Interestingly, a shadow band of half the predicted size was observed by native gel electrophoresis (Figure 2A), and only a single band of the predicted size was seen

by alkaline gel electrophoresis (data not shown) suggesting formation of snapback structures during DNA manipulation or extrusion of the cruciform in vivo.

Second, we turned to aCGH to determine the size of the palindromic duplications. aCGH confirmed loss of distal sequence on Ch V and also indicated a duplication of sequence immediately adjacent to the break point; the breakpoints were consistent with the PCR mapping results (Figures 2B–2D). One clone from the WT strain (8%), seven of nine (78%) *sae2*Δ clones, and nine of ten (90%) *rfa1-t33 sae2*Δ clones analyzed had inversion duplications. Three of the seven inversion duplications recovered from the *sae2*Δ mutant exhibited a ''fading'' duplication (class II): sequences immediately adjacent to the breakpoint were present at 2X but exhibited a gradient of 2X to 1X copy number over an ~70-kb region (Figure 2C), thus giving rise to variable Ch V sizes by PFGE (Figure 1C). Passage of a single class II inversion duplication clone and isolation of single colonies confirmed that the Ch V remains unstable through many generations, but some single colonies isolated did stabilize to form a discrete-sized Ch V (data not shown). The chromosome end may be protecting essential genes by formation of palindromes, as reported previously for survival of recombination and telomerase defective cells (Maringele and Lydall, 2004), and some of these may eventually be stabilized by de novo telomere addition.

Inversion Duplications Require a Secondary Invasion to Stabilize the Chromosome

Many of the GCR clones with an inversion duplication of Ch V had a duplication of another genomic region from the telomere to an internal site (class I) (Figure 2B), suggesting that a secondary event is required to form a stable chromosome by acquisition of a telomere (Pennaneach and Kolodner, 2009). Four of the seven inversion duplications analyzed from the *sae2*Δ mutant and the single event from WT were composed of sequences from the breakpoint to the Ty1-containing *ura3-52* locus (located 76–83 kb away) and were associated with a duplication of another chromosome arm bounded by a Ty1-related element (Ty or delta element) and a telomere. All of the inversion duplications found in the *rfa1-t33 sae2*Δ mutant contained a duplication of another genomic region. Eight of the *rfa1-t33 sae2*Δ clones had an inverted duplication to the *ura3-52* locus associated with a secondary duplication initiated at a Ty1-related element; the remaining clone had an inverted duplication up to a serine tRNA (51 kb) associated with a duplication from an identical serine tRNA present on Ch IV to the telomere. GCRs found in other studies frequently involve repetitive elements, such as delta sequences, but tRNAs have rarely been observed at breakpoint junctions (Fischer et al., 2000; Lemoine et al., 2005; Mieczkowski et al., 2006; Narayanan et al., 2006; Paek et al., 2009). The serine tRNA is only 84 nucleotides in length, considerably shorter than delta (330 bp) and Ty elements (6 kb). The spectra of GCRs recovered from WT and mutant cells are shown in Figure 3A.

Inversion Duplications Are Mediated by Short Inverted Repeats

Inversion duplications can be formed by end joining between two replicated broken sister chromatids or result from intra-strand annealing between short inverted repeats to form a fold-back structure (Marotta et al., 2013). To determine the sequence at the breakpoint of the inversion duplications, we treated the genomic DNA with sodium bisulfite to deaminate the cytosines and thus disrupt the palindrome sufficiently to allow for PCR amplification and DNA sequencing (Rattray, 2004). We found 5- to 9-bp inverted repeats separated by 3- to 12-bp spacer sequences present at the center of the inverted duplications (Table S1). Breakpoints were distributed throughout the 11-kb region between *CAN1* and *PCM1* with some clustering around the *CAN1* locus (Table S1), in agreement with a previous study (Putnam et al., 2005). These data support the hypothesis that inversion duplications in *sae2*Δ derivatives initiate by intra-strand annealing at short inverted repeats followed by gap filling and ligation to create a hairpin-capped end. Replication of the hairpin-capped chromosome would yield a dicentric chromosome that could be broken at mitosis and the end healed by a secondary recombination event or telomere addition (Figure 3B).

Higher-Order Amplifications Observed in *sae2*Δ *rfa1-t33* GCRs

Gene amplifications observed in cancers often have more than a single genomic duplication; some genes are amplified many fold (Kitada and Yamasaki, 2007, 2008; Marotta et al., 2012; Neiman et al., 2008; Tanaka and Yao, 2009). Interestingly, three of nine GCRs with an inverted duplication recovered from the *rfa1-t33 sae2*Δ mutant contained a >2-fold amplification of the region adjacent to the break site (Figures 2D and S3). The clone shown in Figure 2D is estimated to have seven copies of the 49-kb region adjacent to the breakpoint by aCGH hybridization and qPCR. Based on the predicted size of Ch V, and the intensity of hybridization with the *PCM1* probe, the amplification is intrachromosomal. This finding suggests more than one round of palindromic gene amplification, and BFB cycles occurred to generate a higher-order amplification (Figure 3B).

Inversion Duplications Are the Primary Class of GCRs Recovered from *mre11-H125N* Derivatives

Several studies have shown that loss of the Mre11 nuclease via the *mre11-D56N* or *mre11-H125N* mutations results in stabilization of hairpin-capped ends and palindromic duplications (Chen et al., 2013; Lobachev et al., 2002; Moreau et al., 1999; Rattray et al., 2001). However, palindromic duplications were not recovered from the *mre11-H125N* mutant using a variation of the GCR assay used here, even though they were identified as the main class of GCRs in the *sae2*Δ mutant (Putnam et al., 2014). Because the *rfa1-t33* mutation enhances recovery of palindromic duplication in the *sae2*Δ background, we expected a similar outcome in the absence of the Mre11 nuclease. The rate of GCRs was increased by 13- and 13,000-fold in the *mre11-H125N* and *mre11-H125N rfa1-t33* mutants, respectively, relative to WT, similar to the increases found for the *sae2*Δ derivatives (Figure 1B; Table 1). Like the *sae2*Δ derivatives, most of the *mre11-H125N* and *mre11-H125N rfa1-t33* clones exhibited an expanded Ch V by PFGE and an inverted duplication adjacent to the breakpoint (Figure S4). These data support the hypothesis that the Mre11

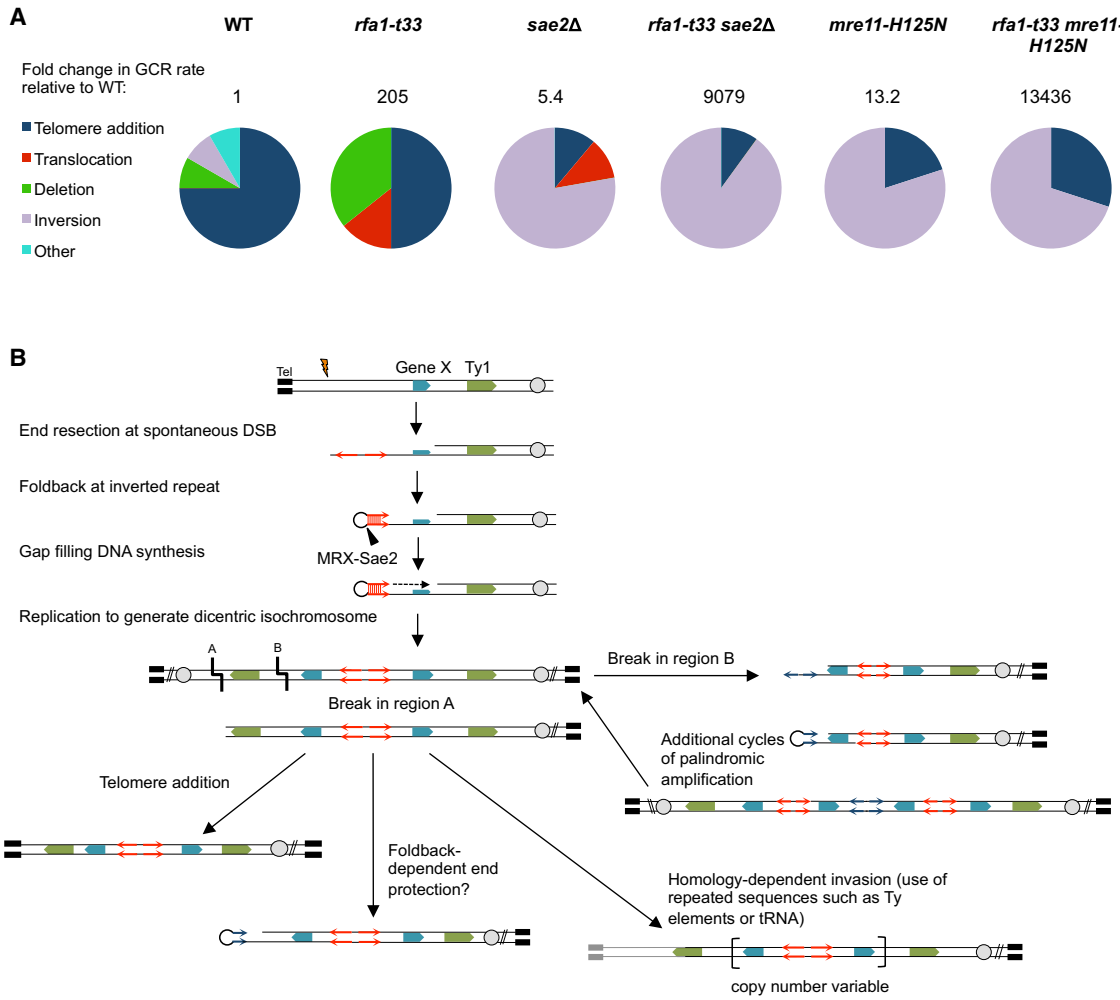

Figure 3. Summary of GCR Data and Model for Palindromic Gene Duplication

(A) The increase in the GCR rate for all of the mutants relative to WT and the spectrum of events recovered from each genotype are shown.

(B) A spontaneous DSB centromere distal to Gene X initiates rearrangement. A foldback in the 3′ single-stranded DNA tail formed by end resection primes DNA synthesis, and the 3′ end is ligated to the resected 5′ end to form a hairpin-capped end. Replication results in a dicentric isochromosome that is broken at mitosis and undergoes additional cycles of foldback priming, telomere addition, or recombination between repeated sequences. A foldback might also stabilize the end to prevent degradation and checkpoint activation. Gray circles, centromeres; thick black lines, telomeres. See also Figures S3 and S4 and Table S1.

nuclease, in conjunction with Sae2, cleaves foldback structures to prevent palindromic duplications. There are two possible explanations for the discrepancy between our results and those of Putnam et al. (2014). First, we used a slightly different GCR assay, and, second, we created a knockin allele of *mre11-H125N* instead of expressing the mutant allele from a plasmid in an *mre11*Δ strain.

DISCUSSION

Foldback priming at resected DSBs is one of the mechanisms proposed to drive palindromic gene duplication (Tanaka and Yao, 2009). Inverted duplications are a rare class of GCRs in WT cells but are the major class of events recovered from *sae2*Δ and *mre11-H125N* mutants, and the frequency of their formation is increased by 50- to 130-fold relative to WT. Although RPA plays an important role in preventing annealing between microhomologies that can lead to foldback structures (Chen et al., 2013; Deng et al., 2014), no inverted duplications were found among the 14 GCR events analyzed from the *rfa1-t33* hypomorphic mutant. However, in the context of Sae2 or Mre11 nuclease deficiency, *rfa1-t33* caused a >1,000-fold increase in the rate of inversion duplications. These data are consistent with the model that RPA normally removes foldback structures and when they do occasionally arise the Mre11 endonuclease and Sae2 efficiently cleave them to prevent formation of inverted duplications.

Palindromic duplications are a major threat to genomic stability because they act as fragile sites and stimulate further amplification and chromosome rearrangements (Lemoine et al., 2005; Narayanan et al., 2006; Tanaka and Yao, 2009). Therefore, the timely removal of foldbacks is essential to

preserve genome integrity and could be one of the main cellular functions for the Mre11 nuclease and Sae2. CtIP (the functional ortholog of Sae2 in vertebrates) and the Mre11 nuclease are required for recombination induced at a hairpin-forming sequence in human cells, and SbcCD, the ortholog of the MR complex, destabilizes palindromes in *E. coli* suggesting hairpin cleavage is evolutionarily conserved (Eykelenboom et al., 2008; Wang et al., 2014).

Of the palindromic duplications observed in *sae2*Δ and *mre11-H125N* mutants, half were stabilized by a secondary rearrangement to acquire a telomere. We propose the dicentric isochromosome generated by replication of the hairpin-capped Ch V is broken between the two centromeres in the vicinity of the Ty1 element at the *ura3* locus (Lopez et al., 2015); then, the Ty or delta element is used for recombination with a Ty1 or delta element elsewhere in the genome (Figure 3B). Chromosome rearrangements mediated by Ty or delta elements have been reported in many other yeast studies, in particular, to stabilize dicentric chromosomes (Lemoine et al., 2005; Mieczkowski et al., 2006; Narayanan et al., 2006; Pennaneach and Kolodner, 2009; Surosky and Tye, 1985). Although we found a high frequency of GCRs in the *rfa1-t33 sae2*Δ and *rfa1-t33 mre11-H125N* mutants, this is likely to be an underestimate of the global genome instability in these cells. The GCR assay used only detects events occurring in an ~30-kb region of Ch V, and many of the secondary recombination events would not generate a viable product.

Short inverted repeats were identified by DNA sequencing at the breakpoints of the palindromic duplications characterized in *sae2*Δ GCR clones. The inverted repeats vary in size from 5 to 9 bp with 1- to 2-bp mismatches and are separated by 2–12 bp. Half of the 12 breakpoints sequenced utilized two sequences, which are the longest if mismatches are included, whereas the other six are unique. All of the palindromic junctions analyzed from *sae2*Δ and *rad50*Δ mutants in a previous study were formed at inverted repeats of 4–6 bp separated by 2–8 bp (Rattray et al., 2005). In contrast, the breakpoints of inverted duplications from *tel1*Δ mutants had inverted repeats of similar sizes to those identified in this study, but with longer spacers (25–44 bp) (Putnam et al., 2014). We speculate that Mre11 and Sae2 recognize and/or cleave foldbacks with short spacers; perhaps other structure-selective nucleases regulated by Tel1 can cleave long ssDNA loops.

Based on the properties of Mre11, Sae2, and RPA^{t33}, intrastrand annealing to form a foldback is a logical mechanism to explain the palindromic duplication rearrangements. We speculate the initiating event is a resected DSB but cannot exclude the possibility of annealing between the leading nascent strand and lagging strand template at a stalled replication fork linking the leading to the lagging strand (Figure S5), as suggested in previous studies (Brewer et al., 2011; Paek et al., 2009). Fork reversal could then lead to a hairpin-capped end, a substrate for MRX-Sae2 cleavage. It is unlikely that inversion duplications are created by MMEJ between replicated broken sister-chromosomes because MMEJ occurs at a high frequency in the *rfa1-t33* mutant, yet we do not observe inversion duplications in the single mutant. Furthermore, an MMEJ mechanism would not explain why palindromic duplications are preferentially recovered from *sae2Δ* and *mre11-H125N* mutants. We argue that it is the hairpin opening activity of Mre11 and Sae2 that prevents formation of inversion duplications.

There are several arguments that our observations are relevant to the mechanisms of carcinogenesis. First, as described in the Introduction, palindromic insertions are a common type of genetic rearrangement in certain classes of tumors. For example, 16% of the chromosome rearrangements in metastatic pancreatic tumors are palindromic duplications compared to 2% of chromosome rearrangements in breast tumors (Campbell et al., 2010). Second, germline mutations in *NBN* (encoding Nbs1/Xrs2) result in the cancer-prone Nijmegen Breakage Syndrome (Thompson and Schild, 2002), and mutations in *RAD50* are associated with an increased risk of familial breast cancer (Walsh and King, 2007). Third, mutations in *RPA* and *MRE11A* genes are found in various classes of sporadic tumors. For example, biallelic mutations of *RPA1* were found in a pancreatic cancer study (Waddell et al., 2015). We examined data from the Broad Institute Cancer Genome Atlas Genome Data Analysis Center (http://gdac.broadinstitute.org/) for significant over-representation of mutations in *RPA1-3*, *MRE11A*, *NBN*, *RAD50*, and *RBBP8/CtIP* in various types of tumors. Both *MRE11A* and *RPA3* were significantly over-represented (p values of 0.016 and 0.009, respectively) among colon adenocarcinomas, and *RPA3* was over-represented ($p = 0.008$) among colorectal adenocarcinomas. A more convincing association between our yeast observations and cancer data would be a demonstration that tumors with mutations in *RPA1-3*, and/or members of the *MRN* complex are associated with higher frequencies of palindromic duplications than observed in tumors with other types of mutations. To our knowledge, such an association has not yet been made.

EXPERIMENTAL PROCEDURES

Yeast strain construction and cell culture were performed using standard methods. Fluctuation assays to determine the rate of GCRs, PCR mapping, and amplification of the junctions were performed as previously described (Putnam and Kolodner, 2010). For physical analysis of inversion duplications, 3 μg of genomic DNA was digested with 20 units of the indicated restriction endonucleases, separated by gel electrophoresis and transferred to Biobond-Plus nylon membrane (Sigma) for hybridization. Samples for PFGE were prepared and analyzed following a published protocol (Argueso et al., 2008). Genomic DNA was extracted from agarose plugs and labeled for microarray hybridization as previously described (Zhang et al., 2013). For bisulfite sequencing, genomic DNA was first treated with the EpiMark Bisulfite Conversion kit (New England Biolabs) and then PCR amplified using EpiMark Hot Start Taq DNA Polymerase (New England Biolabs) according to the manufacturer's instructions. Detailed information regarding methodology and associated references are available in the Supplemental Experimental Procedures.

SUPPLEMENTAL INFORMATION

Supplemental Information includes Supplemental Experimental Procedures, five figures, and one table and can be found with this article online at http://dx.doi.org/10.1016/j.molcel.2015.09.027.

ACKNOWLEDGMENTS

We thank R.D. Kolodner for gifts of yeast strains and plasmids, J.L. Argueso for advice on PFGE, and D. Gordenin for advice on looking for cancer-associated

mutations. This study was supported by grants from the NIH (R01 GM041784 and P01 CA174653 to L.S.S. and R01 GM24110 and GM52319 to T.D.P.).

Received: May 20, 2015
Revised: August 20, 2015
Accepted: September 28, 2015
Published: November 5, 2015

REFERENCES

Argueso, J.L., Westmoreland, J., Mieczkowski, P.A., Gawel, M., Petes, T.D., and Resnick, M.A. (2008). Double-strand breaks associated with repetitive DNA can reshape the genome. Proc. Natl. Acad. Sci. USA *105*, 11845–11850.

Brewer, B.J., Payen, C., Raghuraman, M.K., and Dunham, M.J. (2011). Origin-dependent inverted-repeat amplification: a replication-based model for generating palindromic amplicons. PLoS Genet. *7*, e1002016.

Butler, D.K., Yasuda, L.E., and Yao, M.C. (1996). Induction of large DNA palindrome formation in yeast: implications for gene amplification and genome stability in eukaryotes. Cell *87*, 1115–1122.

Campbell, P.J., Yachida, S., Mudie, L.J., Stephens, P.J., Pleasance, E.D., Stebbings, L.A., Morsberger, L.A., Latimer, C., McLaren, S., Lin, M.L., et al. (2010). The patterns and dynamics of genomic instability in metastatic pancreatic cancer. Nature *467*, 1109–1113.

Cannavo, E., and Cejka, P. (2014). Sae2 promotes dsDNA endonuclease activity within Mre11-Rad50-Xrs2 to resect DNA breaks. Nature *514*, 122–125.

Chen, C., and Kolodner, R.D. (1999). Gross chromosomal rearrangements in Saccharomyces cerevisiae replication and recombination defective mutants. Nat. Genet. *23*, 81–85.

Chen, H., Lisby, M., and Symington, L.S. (2013). RPA coordinates DNA end resection and prevents formation of DNA hairpins. Mol. Cell *50*, 589–600.

Darmon, E., Eykelenboom, J.K., Lincker, F., Jones, L.H., White, M., Okely, E., Blackwood, J.K., and Leach, D.R. (2010). E. coli SbcCD and RecA control chromosomal rearrangement induced by an interrupted palindrome. Mol. Cell *39*, 59–70.

Deng, S.K., Gibb, B., de Almeida, M.J., Greene, E.C., and Symington, L.S. (2014). RPA antagonizes microhomology-mediated repair of DNA double-strand breaks. Nat. Struct. Mol. Biol. *21*, 405–412.

Eykelenboom, J.K., Blackwood, J.K., Okely, E., and Leach, D.R. (2008). SbcCD causes a double-strand break at a DNA palindrome in the Escherichia coli chromosome. Mol. Cell *29*, 644–651.

Fischer, G., James, S.A., Roberts, I.N., Oliver, S.G., and Louis, E.J. (2000). Chromosomal evolution in Saccharomyces. Nature *405*, 451–454.

Gibb, B., Silverstein, T.D., Finkelstein, I.J., and Greene, E.C. (2012). Single-stranded DNA curtains for real-time single-molecule visualization of protein-nucleic acid interactions. Anal. Chem. *84*, 7607–7612.

Kitada, K., and Yamasaki, T. (2007). The MDR1/ABCB1 regional amplification in large inverted repeats with asymmetric sequences and microhomologies at the junction sites. Cancer Genet. Cytogenet. *178*, 120–127.

Kitada, K., and Yamasaki, T. (2008). The complicated copy number alterations in chromosome 7 of a lung cancer cell line is explained by a model based on repeated breakage-fusion-bridge cycles. Cancer Genet. Cytogenet. *185*, 11–19.

Lemoine, F.J., Degtyareva, N.P., Lobachev, K., and Petes, T.D. (2005). Chromosomal translocations in yeast induced by low levels of DNA polymerase a model for chromosome fragile sites. Cell *120*, 587–598.

Lengsfeld, B.M., Rattray, A.J., Bhaskara, V., Ghirlando, R., and Paull, T.T. (2007). Sae2 is an endonuclease that processes hairpin DNA cooperatively with the Mre11/Rad50/Xrs2 complex. Mol. Cell *28*, 638–651.

Lobachev, K.S., Gordenin, D.A., and Resnick, M.A. (2002). The Mre11 complex is required for repair of hairpin-capped double-strand breaks and prevention of chromosome rearrangements. Cell *108*, 183–193.

Lopez, V., Barinova, N., Onishi, M., Pobiega, S., Pringle, J.R., Dubrana, K., and Marcand, S. (2015). Cytokinesis breaks dicentric chromosomes preferentially at pericentromeric regions and telomere fusions. Genes Dev. *29*, 322–336.

Maringele, L., and Lydall, D. (2004). Telomerase- and recombination-independent immortalization of budding yeast. Genes Dev. *18*, 2663–2675.

Marotta, M., Chen, X., Inoshita, A., Stephens, R., Budd, G.T., Crowe, J.P., Lyons, J., Kondratova, A., Tubbs, R., and Tanaka, H. (2012). A common copy-number breakpoint of ERBB2 amplification in breast cancer colocalizes with a complex block of segmental duplications. Breast Cancer Res. *14*, R150.

Marotta, M., Chen, X., Watanabe, T., Faber, P.W., Diede, S.J., Tapscott, S., Tubbs, R., Kondratova, A., Stephens, R., and Tanaka, H. (2013). Homology-mediated end-capping as a primary step of sister chromatid fusion in the breakage-fusion-bridge cycles. Nucleic Acids Res. *41*, 9732–9740.

Mieczkowski, P.A., Lemoine, F.J., and Petes, T.D. (2006). Recombination between retrotransposons as a source of chromosome rearrangements in the yeast Saccharomyces cerevisiae. DNA Repair (Amst.) *5*, 1010–1020.

Mizuno, K., Lambert, S., Baldacci, G., Murray, J.M., and Carr, A.M. (2009). Nearby inverted repeats fuse to generate acentric and dicentric palindromic chromosomes by a replication template exchange mechanism. Genes Dev. *23*, 2876–2886.

Moreau, S., Ferguson, J.R., and Symington, L.S. (1999). The nuclease activity of Mre11 is required for meiosis but not for mating type switching, end joining, or telomere maintenance. Mol. Cell. Biol. *19*, 556–566.

Narayanan, V., Mieczkowski, P.A., Kim, H.M., Petes, T.D., and Lobachev, K.S. (2006). The pattern of gene amplification is determined by the chromosomal location of hairpin-capped breaks. Cell *125*, 1283–1296.

Neiman, P.E., Elsaesser, K., Loring, G., and Kimmel, R. (2008). Myc oncogene-induced genomic instability: DNA palindromes in bursal lymphomagenesis. PLoS Genet. *4*, e1000132.

Paek, A.L., Kaochar, S., Jones, H., Elezaby, A., Shanks, L., and Weinert, T. (2009). Fusion of nearby inverted repeats by a replication-based mechanism leads to formation of dicentric and acentric chromosomes that cause genome instability in budding yeast. Genes Dev. *23*, 2861–2875.

Pennaneach, V., and Kolodner, R.D. (2009). Stabilization of dicentric translocations through secondary rearrangements mediated by multiple mechanisms in S. cerevisiae. PLoS ONE *4*, e6389.

Putnam, C.D., and Kolodner, R.D. (2010). Determination of gross chromosomal rearrangement rates. Cold Spring Harb. Protoc. *2010*, pdb.prot5492. http://dx.doi.org/10.1101/pdb.prot5492.

Putnam, C.D., Pennaneach, V., and Kolodner, R.D. (2005). Saccharomyces cerevisiae as a model system to define the chromosomal instability phenotype. Mol. Cell. Biol. *25*, 7226–7238.

Putnam, C.D., Pallis, K., Hayes, T.K., and Kolodner, R.D. (2014). DNA repair pathway selection caused by defects in TEL1, SAE2, and de novo telomere addition generates specific chromosomal rearrangement signatures. PLoS Genet. *10*, e1004277.

Rattray, A.J. (2004). A method for cloning and sequencing long palindromic DNA junctions. Nucleic Acids Res. *32*, e155.

Rattray, A.J., McGill, C.B., Shafer, B.K., and Strathern, J.N. (2001). Fidelity of mitotic double-strand-break repair in Saccharomyces cerevisiae: a role for SAE2/COM1. Genetics *158*, 109–122.

Rattray, A.J., Shafer, B.K., Neelam, B., and Strathern, J.N. (2005). A mechanism of palindromic gene amplification in Saccharomyces cerevisiae. Genes Dev. *19*, 1390–1399.

Schmidt, K.H., Pennaneach, V., Putnam, C.D., and Kolodner, R.D. (2006). Analysis of gross-chromosomal rearrangements in Saccharomyces cerevisiae. Methods Enzymol. *409*, 462–476.

Slamon, D.J., Clark, G.M., Wong, S.G., Levin, W.J., Ullrich, A., and McGuire, W.L. (1987). Human breast cancer: correlation of relapse and survival with amplification of the HER-2/neu oncogene. Science *235*, 177–182.

Stephens, P.J., Greenman, C.D., Fu, B., Yang, F., Bignell, G.R., Mudie, L.J., Pleasance, E.D., Lau, K.W., Beare, D., Stebbings, L.A., et al. (2011). Massive

genomic rearrangement acquired in a single catastrophic event during cancer development. Cell *144*, 27–40.

Sugiyama, T., New, J.H., and Kowalczykowski, S.C. (1998). DNA annealing by RAD52 protein is stimulated by specific interaction with the complex of replication protein A and single-stranded DNA. Proc. Natl. Acad. Sci. USA *95*, 6049–6054.

Surosky, R.T., and Tye, B.K. (1985). Resolution of dicentric chromosomes by Ty-mediated recombination in yeast. Genetics *110*, 397–419.

Tanaka, H., and Yao, M.C. (2009). Palindromic gene amplification–an evolutionarily conserved role for DNA inverted repeats in the genome. Nat. Rev. Cancer *9*, 216–224.

Tanaka, H., Tapscott, S.J., Trask, B.J., and Yao, M.C. (2002). Short inverted repeats initiate gene amplification through the formation of a large DNA palindrome in mammalian cells. Proc. Natl. Acad. Sci. USA *99*, 8772–8777.

Thompson, L.H., and Schild, D. (2002). Recombinational DNA repair and human disease. Mutat. Res. *509*, 49–78.

Waddell, N., Pajic, M., Patch, A.M., Chang, D.K., Kassahn, K.S., Bailey, P., Johns, A.L., Miller, D., Nones, K., Quek, K., et al.; Australian Pancreatic Cancer Genome Initiative (2015). Whole genomes redefine the mutational landscape of pancreatic cancer. Nature *518*, 495–501.

Walsh, T., and King, M.C. (2007). Ten genes for inherited breast cancer. Cancer Cell *11*, 103–105.

Wang, H., Li, Y., Truong, L.N., Shi, L.Z., Hwang, P.Y., He, J., Do, J., Cho, M.J., Li, H., Negrete, A., et al. (2014). CtIP maintains stability at common fragile sites and inverted repeats by end resection-independent endonuclease activity. Mol. Cell *54*, 1012–1021.

Yasuda, L.F., and Yao, M.C. (1991). Short inverted repeats at a free end signal large palindromic DNA formation in Tetrahymena. Cell *67*, 505–516.

Zhang, H., Zeidler, A.F., Song, W., Puccia, C.M., Malc, E., Greenwell, P.W., Mieczkowski, P.A., Petes, T.D., and Argueso, J.L. (2013). Gene copy-number variation in haploid and diploid strains of the yeast Saccharomyces cerevisiae. Genetics *193*, 785–801.

Molecular Cell

Supplemental Information

Mre11-Sae2 and RPA Collaborate to Prevent Palindromic Gene Amplification

Sarah K. Deng, Yi Yin, Thomas D. Petes, and Lorraine S. Symington

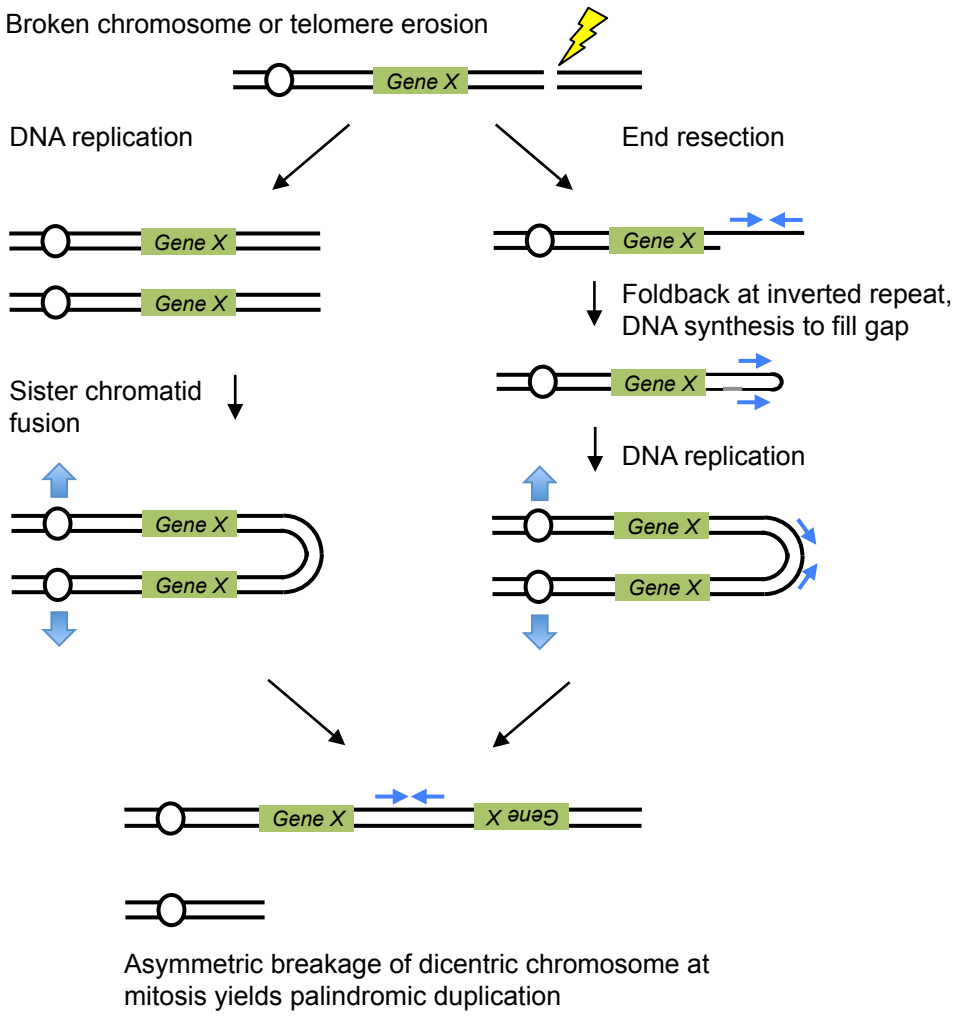

Figure S1, related to Figures 1 and 3. Models for palindromic duplication by break-fusion-bridge cycles.

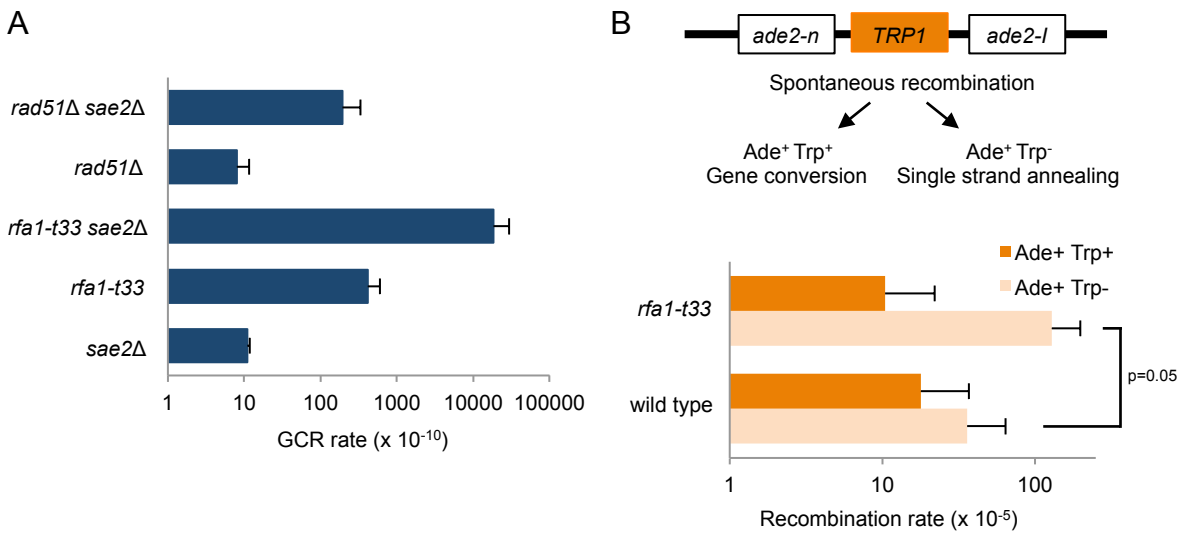

Figure S2, related to Figure 1. Increased GCR rate in the *rfa1-t33* mutant is not due to a recombination defect.
(A) GCR rates for the indicated genotypes. The rates shown for *rad51*Δ and *rad51*Δ *sae2*Δ are the average of three and four independent trials, respectively. Error bars indicate standard deviation.
(B) Recombination rates for wild type and *rfa1-t33* strains. The rates shown are the average of three independent trials. Error bars indicate standard deviation.

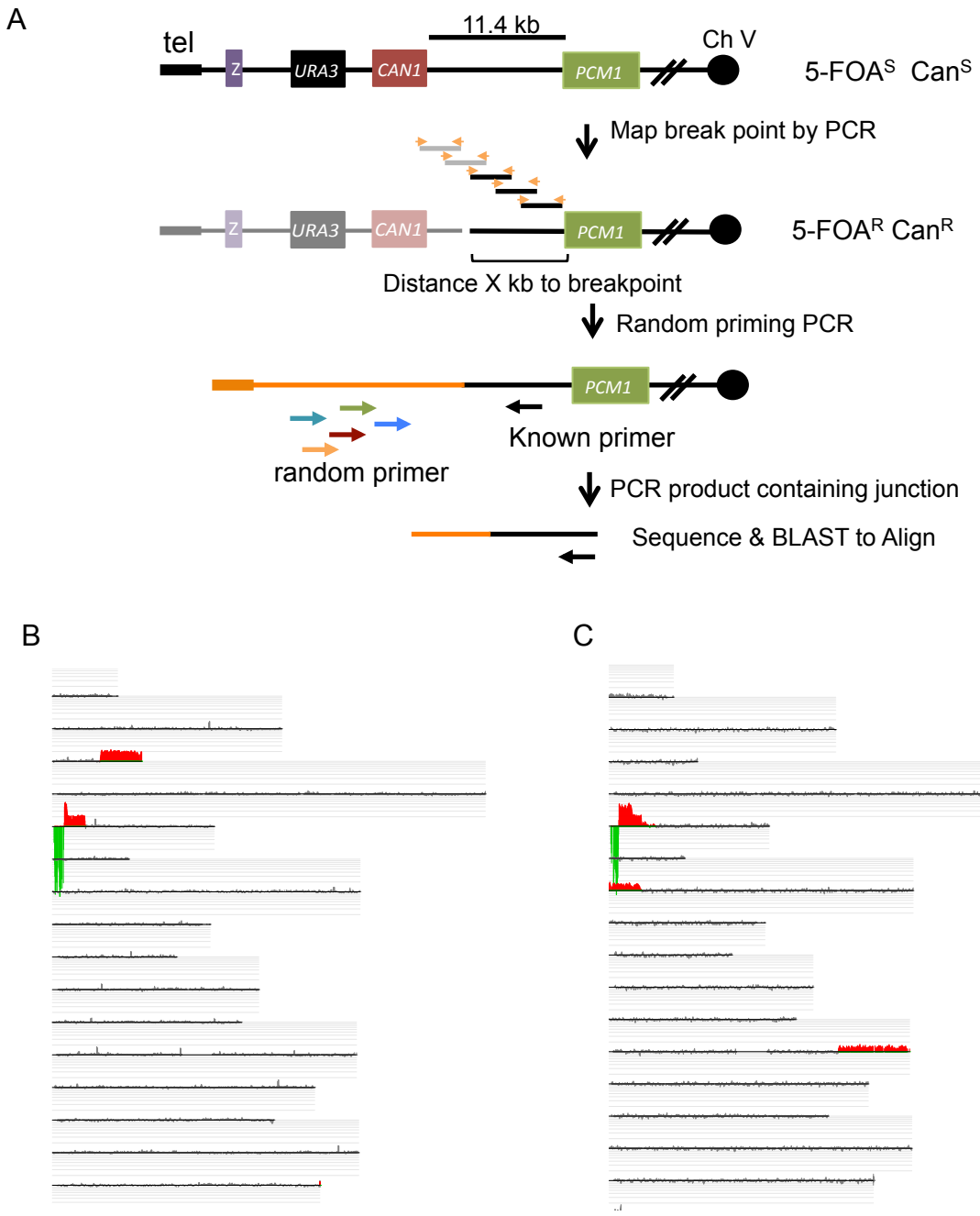

Figure S3, related to Figure 2 and Table 1. Schematic of the PCR assay used to characterize GCRs and CGH of clones with >2-fold amplification of Ch V sequences.
(A) Overlap PCR defines the breakpoint between *CAN1* and *PCM1* then random priming PCR was used to amplify the junction. PCR fragments were sequenced and aligned to the reference genome to define the sequences involved in the rearrangements.
(B) A 10-kb region adjacent to the breakpoint is present in 4 copies.
(C) A 4-fold amplification of a 48 kb region adjacent to the breakpoint. The clone shown represents a mixed population of two clones with the same rearrangement on Ch V associated with distinct secondary rearrangements involving Ch VII and Ch XII (determined by clonal analysis).

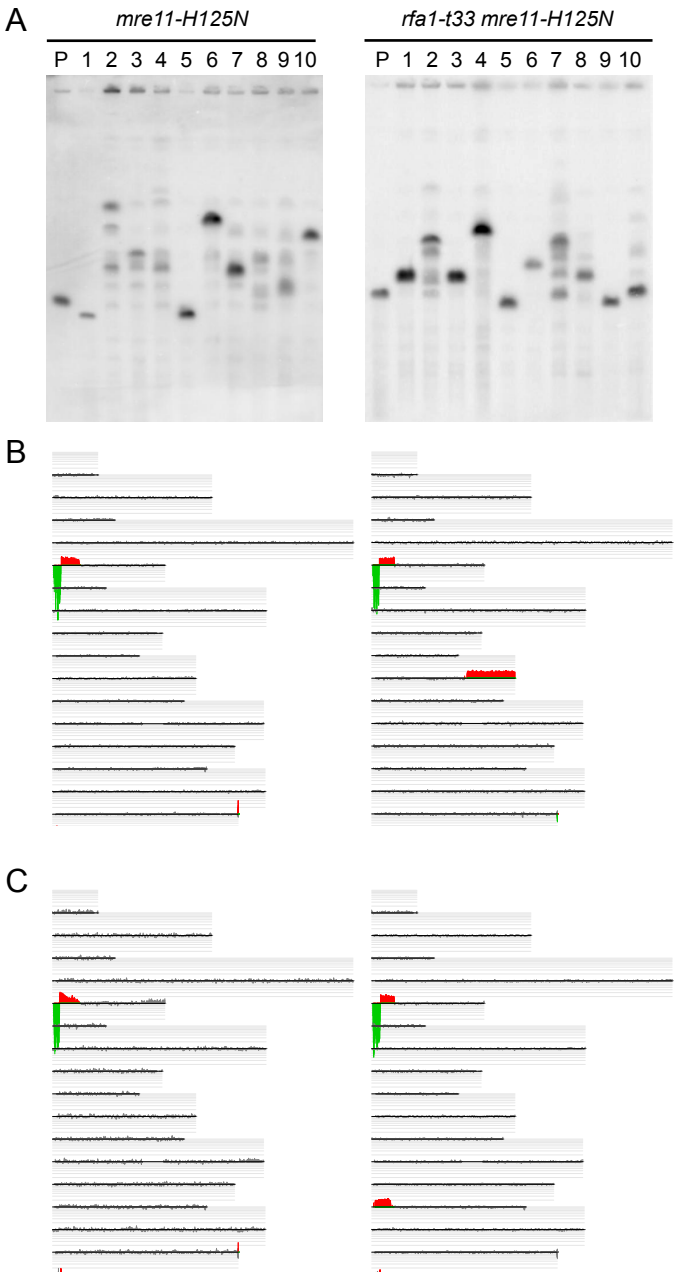

Figure S4, related to Figures 1 and 3. Inversion duplications are recovered from *mre11-H125N* derivatives.
(A) PFGE of independent GCR clones.
(B) Representative microarrays from *mre11-H125N* clones.
(C) Representative microarrays from and *rfa1-t33 mre11-H125N* clones.

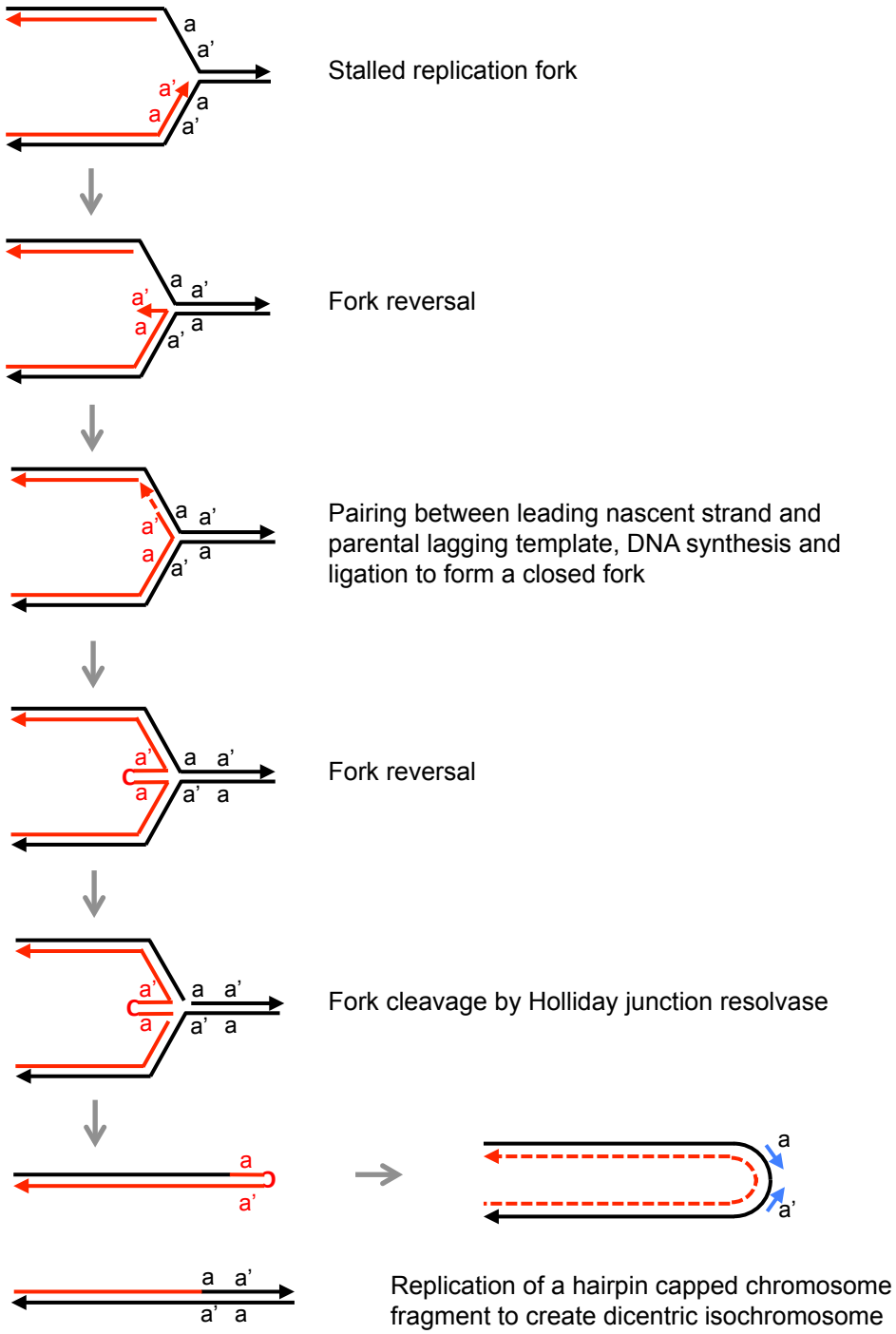

Figure S5, related to Figure 3. Model for generation of a dicentric chromosome by template switching between inverted repeats at a stalled replication fork. a and a' represent short inverted repeats

Table S1, related to Figure 3. Inverted repeats initiate inverted duplications

Relevant genotype	Inverted Repeat Sequence[1]	No. of Events	Ch V coordinate
*sae2*Δ	CCCAGG**ca**CCTGGG	1	32,659
	TATATtTCTG**ttc**CAGAtATATA	1	33,588
	GAGTTT**ctca**AAACTC	1	35,581
	TAA - GCCAC**tgca**GTGGCaTTA	1	42,134
	CGCCA**ctcccgcagtcc**TGGCG	1	42,109
*sae2*Δ *rfa1-t33*	TTCcaGGGCAA**aagtga**TTGCCCaaGAA	4	32,915
	CACTT**gccagt**AAGTG	1	34,006
	CTCgTGGG**cgct**CCCAtGAG	1	41,663
	TATATtTCTG**ttc**CAGAtATATA	1	33,588

[1] Bases in lower case represent mismatches within the inverted repeat, and bases in bold lower case indicate the spacer between inverted repeats.

Supplemental Experimental Procedures

Media, growth conditions and yeast strains. Rich medium (yeast extract-peptone-dextrose, YPD) and synthetic medium (SC) were as described previously (Amberg, 2005). Selection for GCR events was performed using synthetic complete medium without arginine containing 1mg/mL 5-fluoroorotic acid (5-FOA) and 60µg/mL cananvanine (Can) as described (Chen and Kolodner, 1999). Yeast strains are derivatives of RDKY3615 (*MAT***a** *ura3-52 leu2*Δ*1 trp1*Δ*63 his3*Δ*200 lys2*Δ*BglI hom-10 ade2*Δ*1 ade8 yel069::URA3*) and RDK3617 (*MAT***a** *ura3-52 leu2*Δ*1 trp1*Δ*63 his3*Δ*200 lys2*Δ*BglI hom-10 ade2*Δ*1 ade8 yel069::URA3 rfa1-t33*) (Chen and Kolodner, 1999). The *sae2*Δ deletion strains, LSY2706 and LSY2707, were generated by one-step gene-replacement of RDKY3615 and RDKY3617, respectively with *sae2::KanMX* PCR products. The *mre11-H125N* derivatives, LSY3388 and LSY3389, were created by one-step replacement of RDKY3615 and RDKY3617 with *mre11-H125N-NatMX* PCR products. The *rad51*Δ (LSY3441) and *rad51*Δ *sae2*Δ (LSY3442) strains were generated by one-step gene replacement of RDKY3615 and LSY2706 with the XbaI/PstI fragment from the pAM28 plasmid (Rattray and Symington, 1994). Wild type (LSY3449-18A) and *rfa1-t33* (LSY3449-10D) strains bearing the *ade2* direct repeat were generated by crossing appropriate haploids (Mozlin et al., 2008).

GCR assays and PCR mapping. Fluctuation assays to determine the rate of GCRs, PCR mapping and amplification of the junctions were performed as previously described (Putnam and Kolodner, 2010);(Schmidt et al., 2006). Some telomere addition events were identified using a terminal transferase-mediated PCR method (Forstemann et al., 2000). Briefly, terminal transferase (New England Biolabs) was used to add a C-tail to DNA ends. Then, a 5'-(CGGGATCC)G_{18}-3' primer and primer that anneals only adjacent to the breakpoint was used to PCR amplify the region and sequenced. For physical analysis of inversion duplications, 3 µg of genomic DNA was digested with 20 units of the indicated restriction endonucleases,

separated by gel electrophoresis and transferred to Biobond-Plus nylon membrane (Sigma) for hybridization.

PFGE and aCGH. Samples for PFGE were obtained from 7 mL saturated yeast cultures in YPD. Cells were embedded in low-melt agarose and lysed as previously described (Amberg, 2005). Chromosomes were separated by CHEF-DR II Pulsed-Field Electrophoresis system (BioRad) following a published protocol (Argueso et al., 2008). Chromosomes were transferred to nylon membranes and hybridized with a radiolabeled *PCM1* probe to identify Ch V rearrangements. Agarose plugs were melted and the DNA was sonicated, extracted and labeled for microarray hybridization as previously described (Zhang et al., 2013).

Bisulfite sequencing

2 µg of genomic DNA was treated with the EpiMark Bisulfite Conversion kit (New England Biolabs) according to the manufacturers instructions. Bisulfite treated DNA was used for PCR amplification using EpiMark Hot Start Taq DNA Polymerase (New England Biolabs) according to the manufacturers instructions.

Determination of spontaneous mitotic recombination rates: Mitotic recombination rates between *ade2* direct repeats were determined as described previously (Mozlin et al., 2008).

References

Amberg, D.C., Burke, D. J. & Strathern, J. N. (2005). Methods in Yeast Genetics: A Cold Spring Harbor Laboratory Course Manual. Cold spring Harbor Laboratory Press.

Argueso, J.L., Westmoreland, J., Mieczkowski, P.A., Gawel, M., Petes, T.D., and Resnick, M.A. (2008). Double-strand breaks associated with repetitive DNA can reshape the genome.

Proceedings of the National Academy of Sciences of the United States of America *105*, 11845-11850.

Chen, C., and Kolodner, R.D. (1999). Gross chromosomal rearrangements in *Saccharomyces cerevisiae* replication and recombination defective mutants. Nat Genet *23*, 81-85.

Forstemann, K., Hoss, M., and Lingner, J. (2000). Telomerase-dependent repeat divergence at the 3' ends of yeast telomeres. Nucleic acids research *28*, 2690-2694.

Mozlin, A.M., Fung, C.W., and Symington, L.S. (2008). Role of the *Saccharomyces cerevisiae* Rad51 paralogs in sister chromatid recombination. Genetics *178*, 113-126.

Putnam, C.D., and Kolodner, R.D. (2010). Determination of gross chromosomal rearrangement rates. Cold Spring Harb Protoc *2010*, pdb prot5492.

Rattray, A.J., and Symington, L.S. (1994). Use of a chromosomal inverted repeat to demonstrate that the RAD51 and RAD52 genes of *Saccharomyces cerevisiae* have different roles in mitotic recombination. Genetics *138*, 587-595.

Schmidt, K.H., Pennaneach, V., Putnam, C.D., and Kolodner, R.D. (2006). Analysis of gross-chromosomal rearrangements in *Saccharomyces cerevisiae*. Methods Enzymol *409*, 462-476.

Zhang, H., Zeidler, A.F., Song, W., Puccia, C.M., Malc, E., Greenwell, P.W., Mieczkowski, P.A., Petes, T.D., and Argueso, J.L. (2013). Gene copy-number variation in haploid and diploid strains of the yeast *Saccharomyces cerevisiae*. Genetics *193*, 785-801.